

Destruction of Magnetization during TOCSY Experiments Performed under Magic Angle Spinning: Effect of Radial B_1 Inhomogeneities

Martial Piotto,* Maryse Bourdonneau,* Julien Furrer,† Alberto Bianco,‡ Jesús Raya,† and Karim Elbayed†

†Institut de Chimie, UMR 7510 CNRS-Bruker, Université Louis Pasteur, BP 296, F-67008 Strasbourg Cedex, France; *UMR 7510 CNRS-Bruker, 34, rue de l'industrie, F-67166 Wissembourg, France; and ‡Institut de Biologie Moléculaire et Cellulaire UPR 9021 CNRS, 15 rue René Descartes, F-67000 Strasbourg, France

Received August 4, 2000; revised December 24, 2000

TOCSY experiments performed on liquid-like samples under magic angle spinning conditions can exhibit some very peculiar behavior. In the most extreme cases, an almost complete loss of magnetization is observed. The intensity of the effect depends essentially on the ratio of the radiofrequency field strength to the speed of rotation of the sample. It is shown in this study that the periodic modulation of the B_1 field in the course of the sample rotation is responsible for this effect. © 2001 Academic Press

Key Words: HRMAS; B_1 inhomogeneity; solenoid coil; TOCSY; MLEV-16; DIPSI-2.

High-resolution magic angle spinning (1, 2) (HRMAS) is an exciting new technique allowing the characterization by NMR of inhomogeneous compounds with liquid-like dynamics (3). The domain of application ranges from the study of organic molecules and peptides bound to a swollen solid resin support (4–11) to polymers, lipids (12), and human and animal tissues (13, 14).

The basic principle of HRMAS is to spin the sample at the magic angle (54.7°) in order to remove the line broadening effect of large differences in magnetic susceptibilities present in inhomogeneous compounds. This results in a dramatic sharpening of the NMR signals whose linewidth is determined essentially by the relaxation properties of the system and by the amount of anisotropic magnetic susceptibility (15). Under such conditions, the sample behaves very much like a liquid and standard liquid pulse sequences can be employed.

HRMAS can also be used to study quantity limited liquid state samples by allowing the entire sample to be positioned within the radiofrequency (RF) coil of the probe, therefore increasing the sensitivity of the experiment (16). The strong magnetic susceptibility discontinuities present at the liquid/rotor interface will be averaged out by MAS leading to spectra with a very high resolution.

Under HRMAS conditions, the sample behaves very much like a liquid sample in a high-resolution probe and standard liquid state NMR pulse sequences like NOESY (17), TOCSY (18), HSQC (19), and HMBC (20) can be used. The method is

extremely powerful and reliable, and provides a fast access to structure elucidation using established recipes.

However, at an early stage, unexpected effects were noted in TOCSY spectra recorded under MAS. These effects varied from strong phase distortions (M. Piotto and M. Bourdonneau, unpublished results) to an almost complete disappearance of the magnetization (21). In order to overcome these problems, the use of adiabatic mixing pulses (22), in place of the standard MLEV-16 sequence, has been proposed (21).

Since these phenomena are both intriguing and potentially very harmful, we decided to investigate their origin. In order to reach this purpose, the spectra resulting from the first increment of an MLEV-16 (23) experiment were recorded at different spinning speeds on the tetrapeptide Ala-Ile-Gly-Met bound to a Wang resin (Fig. 1). A constant γB_1 field of 8 kHz was chosen for the MLEV-16 sequence, which corresponds to the value classically used at moderate B_0 field strengths. The results clearly show a strong dependence on the spinning rate with a striking destruction of the magnetization at 4 kHz and a strong decrease in intensity at 2 and 6 kHz.

The maximum expected intensity is reached only at a speed of 8 kHz. In order to evaluate the time evolution of the magnetization, 1D MLEV-16 spectra were recorded at 4 and 8 kHz as a function of the number of MLEV-16 cycles. As can be seen in Fig. 2, the difference in the results obtained at the two spinning frequencies is striking. While the intensity is normally preserved at 8 kHz, just a single MLEV-16 cycle is sufficient to attenuate the intensity of the signal by a factor of 2.5 at 4 kHz.

Since the tetrapeptide studied is a fairly complex sample that can contain some residual dipolar or chemical shift anisotropy (CSA) interactions (24), a sample of sucrose in D_2O was subjected to exactly the same experiment. This sample is a true liquid and contains a HDO peak with no scalar interactions. The results obtained on the sucrose molecule and on the HDO line (data not shown) reveal the same abnormal behavior as that observed for the tetrapeptide. These experimental data allowed us to eliminate the possibility of some unwanted recoupling of dipolar or CSA interactions or some effect of scalar interactions.

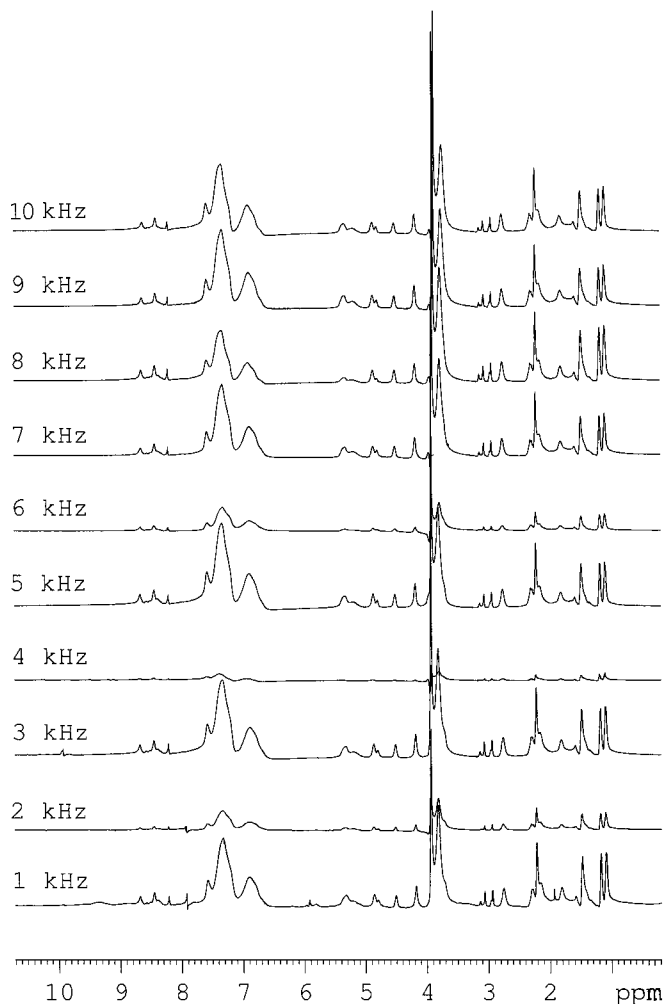


FIG. 1. Proton spectra of the first increment of an MLEV-16 sequence recorded on the tetrapeptide Ala-Ile-Gly-Met bound to a Wang resin and swollen in DMF. The spectra were recorded at different spinning speeds from 1 to 10 kHz. The constant γB_1 field used for the MLEV-16 element was set to 8 kHz and two MLEV-16 cycles, corresponding to a 4-ms mixing time, were applied. Spectra were recorded on a Bruker Avance 500-MHz spectrometer equipped with a 4-mm $^1\text{H}/^{13}\text{C}^2\text{D}$ HRMAS gradient probe.

These considerations led us, in turn, to investigate the possible consequences of variations in the effective B_1 field ($B_{1,\text{eff}} = \sqrt{B_1^2 + \Delta\omega^2}$) in the course of the sample rotation.

As will be seen below, sample rotation can make both the offset $\Delta\omega$ of the spin of interest and the intensity of the B_1 field time-dependent. A sucrose sample, unlike a peptide bound to a resin, is a homogeneous liquid with a uniform magnetic susceptibility. Therefore, only the effects of B_0 field inhomogeneities need to be considered in the following. Upon rotation, a volume element of the sample will be transported through regions with different B_0 values, leading to a time-dependent offset term $\Delta\omega(t)$ (25). To evaluate the magnitude of these inhomogeneities, the linewidth of the HDO line in a spinning and

a nonspinning sample was measured. The results obtained, 0.7 and 15 Hz, respectively, show that the amplitude of these B_0 inhomogeneities is of the order of 15 Hz. When compared to the 8 kHz used for the MLEV-16 mixing, the influence of the B_0 modulation on the intensity of the effective B_1 field is seen to be very small. Moreover, simulations using dipolar fields to represent B_0 inhomogeneities (26) under magic angle rotation (27) do not reproduce the spinning speed dependence observed experimentally for the MLEV-16 spectra.

Turning now to the effect of B_1 inhomogeneities, it is clear that in the course of the rotation, volume elements of the sample will experience different B_1 field values that might seriously affect the outcome of the experiment. This point will be examined in more detail in the following.

The signal variations observed in Fig. 1 as a function of the spinning speed indicate clearly that only radial B_1 inhomogeneities should be considered since axial inhomogeneities would not be affected by a change in the speed of rotation. Another important piece of information contained in the results

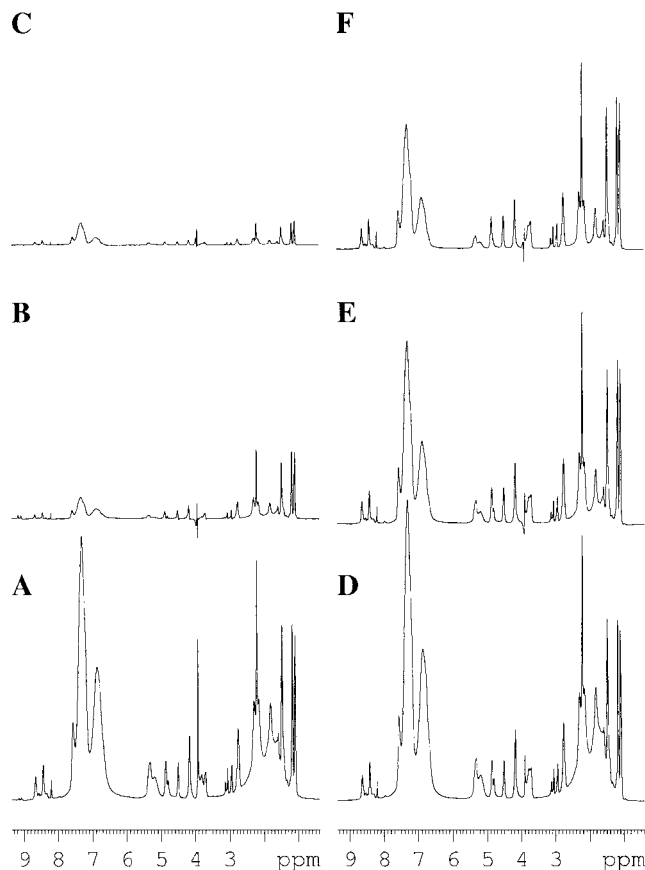


FIG. 2. Evolution of the first increment of an MLEV-16 sequence as a function of mixing time at two different spinning speeds: (A–C) 4 kHz and (D–F) 8 kHz. The spectra were recorded with zero (A, D), one (B, E), and two (C, F) MLEV-16 cycles. A γB_1 field of 8 kHz was used, corresponding to a 2-ms MLEV-16 cycle.

shown in Fig. 1 is that the phenomenon is most pronounced when the speed of rotation is exactly equal to one-half of the B_1 field (i.e., $\omega_r = 4$ kHz). In that case, the period of the rotor is of $250 \mu\text{s}$ which means that during one sample rotation, exactly two elements of the MLEV-16 cycle are executed. Following the conventional nomenclature, these two elements are either $R\bar{R}$, $\bar{R}R$, $\bar{R}\bar{R}$ or RR (where $R = 90_x^\circ - 180_y^\circ - 90_x^\circ$ and $\bar{R} = 90_{-x}^\circ - 180_{-y}^\circ - 90_{-x}^\circ$). In the following, we will focus the discussion on the $R\bar{R}$ element only.

Clearly, if the B_1 field fluctuates in the course of the sample rotation, the $R\bar{R}$ element will no longer return the magnetization to its initial position and the properties of the MLEV-16 sequence will seriously deteriorate. At this point, it is worth remembering that, by design, a solenoid coil can not be made perfectly B_1 homogeneous in its radial plane. Indeed, the wiring of a solenoid is such that a plane perpendicular to the axis of the solenoid is physically not symmetrical. The very nature of the solenoid coil will therefore generate a periodic time-dependent B_1 field in the radial direction upon sample rotation.

On a more quantitative level, the B_1 field can be expressed as a periodic function and, for the purpose of the problem being discussed here, a simple cosine modulation will be assumed. The expression for $\omega_1 = -\gamma B_1$ is given by

$$\omega_1(t) = \omega_{1,0}(1 + a \cos(\omega_r t + \phi)), \quad [1]$$

where $\omega_{1,0}$ is the nominal $\gamma B_{1,0}$ field, ω_r is the speed of rotation, a is a number describing the intensity of the modulation by the inhomogeneity, and ϕ is a phase factor related to the position of the rotor.

The exact meaning of ϕ deserves a more detailed explanation. If, within a given radial plane, one considers a thin circle, the spins at the different positions on that circle will experience the same B_1 modulation but at shifted times. The observed NMR signal within that circle will be the sum over all ϕ values.

To evaluate the effect of this time-dependent B_1 field during the $R\bar{R}$ part of an MLEV-16 cycle, it is necessary to evaluate the six propagators that correspond to the six elements of the $R\bar{R}$ cycle. For an isolated, on-resonance, spin system the following propagators apply:

$$R_{\frac{\pi}{2},+x} = \exp \left[+i \int_0^{\frac{\pi}{2\omega_{1,0}}} \omega_{1,0}(1 + a \cos(\omega_r t + \phi)) dt I_x \right]$$

$$R_{\pi,+y} = \exp \left[+i \int_{\frac{\pi}{2\omega_{1,0}}}^{\frac{3\pi}{2\omega_{1,0}}} \omega_{1,0}(1 + a \cos(\omega_r t + \phi)) dt I_y \right]$$

$$R_{\frac{\pi}{2},+x} = \exp \left[+i \int_{\frac{3\pi}{2\omega_{1,0}}}^{\frac{4\pi}{2\omega_{1,0}}} \omega_{1,0}(1 + a \cos(\omega_r t + \phi)) dt I_x \right]$$

$$R_{\frac{\pi}{2},-x} = \exp \left[+i \int_{\frac{4\pi}{2\omega_{1,0}}}^{\frac{5\pi}{2\omega_{1,0}}} \omega_{1,0}(1 + a \cos(\omega_r t + \phi)) dt (-I_x) \right]$$

$$R_{\pi,-y} = \exp \left[+i \int_{\frac{5\pi}{2\omega_{1,0}}}^{\frac{7\pi}{2\omega_{1,0}}} \omega_{1,0}(1 + a \cos(\omega_r t + \phi)) dt (-I_y) \right]$$

$$R_{\frac{\pi}{2},-x} = \exp \left[+i \int_{\frac{7\pi}{2\omega_{1,0}}}^{\frac{8\pi}{2\omega_{1,0}}} \omega_{1,0}(1 + a \cos(\omega_r t + \phi)) dt (-I_x) \right]. \quad [2]$$

The integration value $\pi/2\omega_{1,0}$ corresponds to the length of a 90° pulse. In the special case where $\pi/2\omega_{1,0} = T_R/8$ (which is equivalent to the condition $\omega_{1,0} = 2\omega_r$), the length of the $R\bar{R}$ cycle precisely matches the period of the sample rotation. This situation is the one observed for $\omega_r = 4$ Hz in Fig. 1 and leads to the maximum effect. Under these conditions, the errors introduced by RF inhomogeneities in the $R\bar{R}$ cycle are applied repetitively and additively during every rotor cycle leading to the observed loss of magnetization.

More precisely, the evolution of the density operator $\sigma(t)$ under the influence of the $R\bar{R}$ cycle under MAS starting with I_y magnetization can be calculated using

$$\sigma(t) = R_{\frac{\pi}{2},-x}^{-1} R_{\pi,-y}^{-1} R_{\frac{\pi}{2},-x}^{-1} R_{\frac{\pi}{2},+x}^{-1} R_{\pi,+y}^{-1} R_{\frac{\pi}{2},+x}^{-1} I_y R_{\frac{\pi}{2},+x} \\ \times R_{\pi,+y} R_{\frac{\pi}{2},+x} R_{\frac{\pi}{2},-x} R_{\pi,-y} R_{\frac{\pi}{2},-x}. \quad [3]$$

In order to grasp some insight into the physical process, the evaluation of Eq. [3] was performed for some selected ϕ values and one $R\bar{R}$ cycle with the program *Mathematica*. ω_r and $\omega_{1,0}$ were set to 4000 and 8000 Hz, respectively, and a value of 10% was chosen for the inhomogeneity contribution a in order to accentuate the phenomenon. The results obtained for the values $\phi = 0, \frac{\pi}{4}, -\frac{\pi}{4}$ are

$$I_y \xrightarrow{\phi=0} I_y$$

$$I_y \xrightarrow{\phi=\frac{\pi}{4}} 0.92I_y - 0.39I_x + 0.00I_z \quad [4]$$

$$I_y \xrightarrow{\phi=-\frac{\pi}{4}} 0.92I_y + 0.39I_x + 0.00I_z.$$

These results show that for a ϕ value of 0, the magnetization is returned exactly to I_y whereas for a ϕ value of $\pi/4$ and $-\pi/4$, the

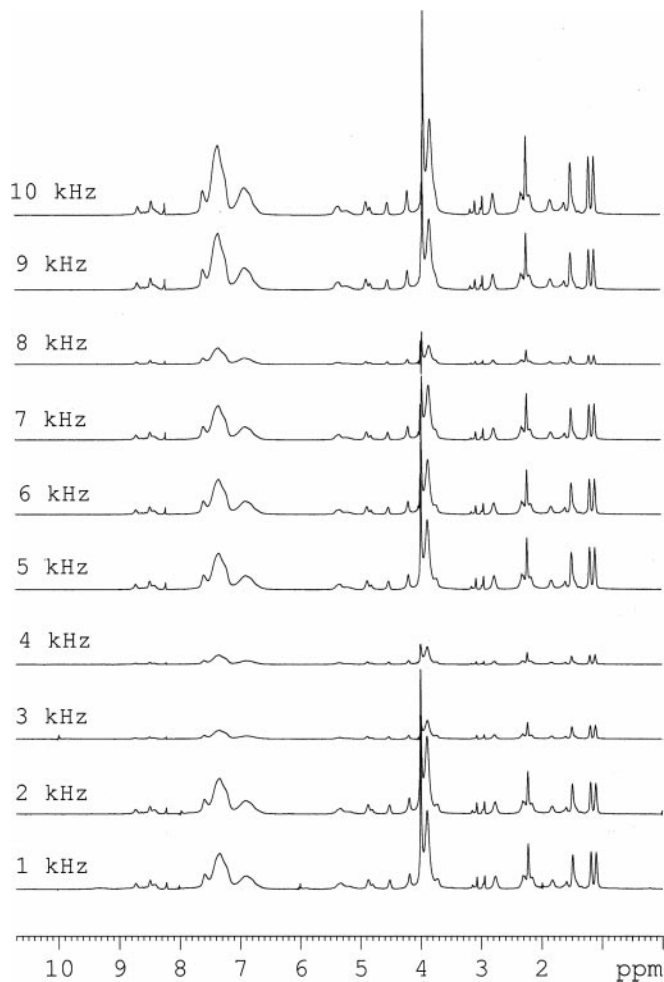


FIG. 3. Proton spectra of the first increment of a DIPSII-2 sequence recorded on the tetrapeptide Ala-Ile-Gly-Met bound to a Wang resin and swollen in DMF. The spectra were recorded at different spinning speeds from 1 to 10 kHz. The constant γB_1 field used for the MLEV-16 element was set to 8 kHz and two DIPSII-2 cycles, corresponding to a 3.6-ms mixing time, were applied.

magnetization evolves in the (x, y) plane in opposite directions. Overall, the effect of the $R\bar{R}$ sequence over a whole set of ϕ values is to spread the magnetization in a slightly tilted (x, y) plane.

The process is of course accentuated when the $R\bar{R}$ cycle is repeated numerous times as in a standard MLEV-16 sequence. The situation is similar to the dephasing caused by a strong B_1 gradient pulse^(28, 29).

The simulation was carried out one step further by subjecting I_y magnetization to two full MLEV-16 cycles and by summing the magnetization over ten ϕ values and six a values to approximate the case of a real rotor. The results (data not shown) reveal that at 8 kHz, the I_y intensity remains almost constant, whereas at 4 kHz, it drops rapidly. These results are in full agreement with the experimental results at 4 and 8 kHz presented in Figs. 1 and 2.

The fact that, at 8 kHz, the MLEV-16 cycle does not produce any appreciable loss of magnetization can be understood the following way: At that frequency an R cycle is equal to exactly one rotor period, which means that the next \bar{R} cycle will be subjected to exactly the same inhomogeneities, therefore returning the magnetization to its initial position.

In order to reproduce with our simulations the intensity drops observed in Fig. 1 at 2 and 6 kHz, a second modulation of the form $\cos(2\omega_r t + 2\phi)$ was added to Eq. [1]. The model used to represent B_1 inhomogeneities requires therefore at least first- and second-order harmonics. In fact, a finer inspection of the ω_r dependence shown in Fig. 1 reveals that additional faster modulations of much lower amplitude are also present which is in agreement with the complexity of the models needed to represent real B_1 fields (25).

The study presented for the MLEV-16 cycle can be extended to more complex mixing schemes. As an example, Fig. 3 shows the results of a DIPSII-2 (30) experiment obtained under the same conditions as Fig. 1. Due to the complexity of the DIPSII-2 mixing scheme, the physical interpretation of the relationship between the B_1 field strength and the speed of rotation is more difficult to comprehend. However, these results clearly indicate that the speed of rotation is an essential parameter to optimize when setting up a TOCSY experiment under MAS conditions.

In conclusion, we have shown that radial B_1 inhomogeneities can generate some spectacular losses of signal when composite pulse sequences like MLEV-16 are applied under magic angle spinning conditions. For an MLEV-16 sequence, this effect is maximum when the speed of rotation of the rotor is equal to one-half the B_1 field. Spinning at frequencies equal to the B_1 field alleviates the problem. For more complex mixing sequences, a careful optimization of the speed of rotation as a function of the B_1 field used is essential.

ACKNOWLEDGMENTS

We thank Baudoin Dillmann for stimulating discussions about the properties of the solenoid coil.

REFERENCES

1. E. R. Andrew, A. Bradbury, and R. G. Eades, *Nature* **182**, 1659 (1958).
2. I. J. Lowe, *Phys. Rev. Lett.* **2**, 285 (1959).
3. G. Lippens, M. Bourdonneau, C. Dhalluin, R. Warras, T. Richert, C. Seetharaman, C. Bouillon, and M. Piotto, *Curr. Org. Chem.* **3**, 147-169 (1999).
4. W. L. Filtch, G. Dettre, C. P. Holmes, J. Scoolery, and P. A. Keiffer, *J. Org. Chem.* **59**, 7955 (1994).
5. R. C. Anderson, M. A. Jarema, M. J. Shapiro, J. P. Stokes, and M. Zilliox, *J. Org. Chem.* **60**, 2650 (1995).
6. R. C. Anderson, J. P. Stokes, and M. J. Shapiro, *Tetrahedron Lett.* **36**, 5311 (1995).
7. P. A. Keiffer, *J. Org. Chem.* **61**, 1558-1559 (1996).
8. I. E. Pop, C. F. Dhalluin, B. P. Déprez, P. C. Melnyk, and G. Lippens, *Tetrahedron* **52**, 12209 (1996).

9. C. Dhalluin, C. Boutillon, A. Tartar, and G. Lippens, *J. Am. Chem. Soc.* **119**, 10494 (1997).
10. R. Jelinek, A. P. Valente, K. G. Valentine, and S. J. Opella, *J. Magn. Reson.* **125**, 185–187 (1997).
11. M. J. Shapiro, J. Chin, R. E. Marti, and M. Jarosinski, *Tetrahedron Lett.* **38**, 1333–1336 (1997).
12. J. D. Gross, P. R. Costa, J. P. Dubacq, D. E. Warschawski, P. N. Lirsac, P. F. Devaux, and R. G. Griffin, *J. Magn. Reson.* **106**, 187–190 (1995).
13. D. Moka, R. Vorreuter, H. Schicha, M. Spraul, E. Humpfer, M. Lipinsky, P. J. D. Foxall, J. K. Nicholson, and J. C. Lindon, *Anal. Commun.* **34**, 107–109 (1997).
14. L. L. Chang, C. L. Lean, A. Bogdanova, and S. C. Wright, *Magn. Reson. Med.* **36**, 653 (1996).
15. K. Elbayed, M. Bourdonneau, J. Furrer, T. Richert, J. Raya, J. Hirschinger, and M. Piotto, *J. Magn. Reson.* **136**, 127–129 (1999).
16. T. M. Barbara, *J. Magn. Reson.* **109**, 265–269 (1994).
17. J. Jeener, B. H. Meier, P. Bachman, and R. R. Ernst, *J. Chem. Phys.* **71**, 4546 (1979).
18. L. Braunschweiler and R. R. Ernst, *J. Magn. Reson.* **53**, 521 (1983).
19. G. Bodenhausen and D. J. Ruben, *Chem. Phys. Lett.* **69**, 185 (1980).
20. A. Bax and M. F. Summers, *J. Am. Chem. Soc.* **108**, 2093 (1986).
21. M. Delepierre, A. Porchnicka-Chalufourc, J. Boisbouvier, and L. D. Possani, *Biochemistry* **38**, 16756 (1999).
22. E. Kupce, P. Schmidt, M. Rance, and G. Wagner, *J. Magn. Reson.* **135**, 361 (1998).
23. M. H. Levitt and R. Freeman, *J. Magn. Reson.* **33**, 473 (1979).
24. J. Furrer, J. Raya, J. Hirschinger, M. Piotto, M. Bourdonneau, A. Bianco, G. Guichard, J.-P. Briand, and K. Elbayed, submitted for publication.
25. D. Hoult, *Prog. NMR Spectrosc.* **12**, 41 (1978).
26. A. N. Garroway, *J. Magn. Reson.* **49**, 168–171 (1982).
27. E. R. Andrew, Magic angle spinning, in “Encyclopedia of NMR” (D. M. Grant and R.K. Harris, Eds.), pp. 2891–2901, Wiley, Chichester, United Kingdom (1996).
28. J. Brondeau, D. Boudot, P. Mutzenhardt, and D. Canet, *J. Magn. Reson.* **100**, 611 (1992).
29. W. E. Maas, F. Laukien, and D. Cory, *J. Magn. Reson.* **103**, 115 (1993).
30. A. J. Shaka, C. J. Lee, and A. Pines, *J. Magn. Reson.* **77**, 274 (1988).